Sum rules and determination of exciton coupling using absorption and circular dichroism spectra of biological polymers

Alexander L. Burin[a,1], Michael E. Armbruster[a], Mahesh Hariharan[b], and Frederick D. Lewis[b]

[a]Department of Chemistry, Tulane University, New Orleans LA 70118; and [b]Department of Chemistry, Northwestern University, Evanston IL 60208

Edited by George C. Schatz, Northwestern University, Evanston, IL, and approved November 25, 2008 (received for review August 27, 2008)

Optical spectra of biological polymers contain important information about their structure and function in living organisms. This information can be accessed by extracting an optical interaction of monomers, i.e., their exciton coupling, from experimental data. This coupling is sensitive to molecular structure, geometry, and conformation and can be used to characterize them. However, the accurate determination of exciton coupling in important biological molecules is difficult because inhomogeneous broadening smears out the monomer interaction. We suggest a way to overcome this problem by applying exact sum rules. These sum rules are derived by establishing a straightforward relationship between integral characteristics of absorption and circular dicroism spectra, and exciton coupling. Exciton coupling between AT pairs in native DNA conformation is estimated by applying these sum rules to DNA hairpin optical spectra as $V_0 \sim 0.035$ eV in agreement with the earlier numerical calculations.

DNA | photons

Optical properties of biological molecules contain important information about their structure and function (1–5). Proteins and DNA are composed of interacting monomers, i.e., amino acids or base pairs. Interactions of monomer electronic excited states lead to a quantum mechanical delocalization of electronic excitation (exciton). This delocalization affects absorption and circular dichroism (CD) spectra and leads to the fluorescent resonant energy transfer between different monomers or molecules. Based on optical measurements one can attempt to determine exciton coupling strengths of monomers serving as chromophores. This coupling strength depends on the distance between monomers and their relative orientation (6, 7). Thus, by observing changes in DNA and protein optical spectra during chemical and biological processes one can investigate their function in living organisms. In addition to biological applications, exciton coupling is important in optical nanosystems involving DNA and proteins (8, 9).

Optical spectra of biological molecules are crucially sensitive to the interaction with their natural environment of highly polar solvent, i.e., water. Therefore, it is difficult to extract information about monomer interaction by using optical spectra, which are smeared out by the solvent-induced inhomogeneous broadening. Indeed, positions and orientations of water molecules with respect to each solute molecule differ from each other leading to quasi-random shifts of electronic excitation energies. These quasi-random shifts contribute to the inhomogeneous spectral broadening $W > 0.1$ eV, which usually exceeds an exciton coupling strength $V_0 < 0.1$ eV (10). Therefore, this broadening can smear out the change of spectra associated with the monomer interaction, which is sensitive to molecular conformation and geometry.

Despite the large inhomogeneous broadening, absorption and CD spectra are still sensitive to interactions of monomers (7). For instance, optical absorption spectra of DNA hairpins made of identical *AT* base pairs demonstrate the blue shift in the energy corresponding to the absorption spectrum maximum with the number of monomers n (11, 12). Under certain conditions this shift can be used to determine the exciton coupling strength V_0, as was recently demonstrated for DNA hairpins (10). A CD spectrum can be even more sensitive to exciton coupling V_0 than an absorption spectrum, particularly in polymers made of planar monomers located parallel to each other as in DNA. Then the circular dichroism originates entirely from exciton coupling (13) (see also refs. 14 and 15 and references therein), so in contrast to absorption this coupling entirely determines a CD spectrum. However, it is hard to extract exciton coupling from a CD spectrum because of its complicated shape sensitive to the details of inhomogeneous broadening.

In this article we propose an efficient way to overcome the effect of inhomogeneous broadening by using the exact sum rules for CD spectra. These sum rules are based on the Van Vleck theory (16) and its later extension to absorption spectra (17) (see also ref. 18). We show that if the excited electronic state of monomers under consideration is well separated from other states, then one can express the exciton coupling of neighboring monomers V_0 in terms of energy-dependent absorbance $A(E)$ and ellipticity angle $\Theta(E)$ characterizing CD strength (expressed in radians)

$$V_0 = \frac{2}{\ln(10)} \frac{n}{n-1} \frac{\hbar c}{d n_r \sin(\varphi)} \frac{\int_{-\infty}^{+\infty} dE \frac{\Theta(E)}{E}}{\int_{-\infty}^{+\infty} dE \frac{A(E)}{E}}, \qquad [1]$$

where n is the number of monomers, φ is the angle between dipole moments of adjacent monomers, d is the distance between them, and n_r is the refractive index of the material. This equation applies to a linear system only. The interaction between nonneighboring monomers is ignored because of its rapid decrease with the distance. In this article we derive general expressions for polymer absorption and CD spectra, define the most general model for the molecule affected by the inhomogeneous broadening, derive exact relationships (e.g., Eq. **1**) and apply them to determine exciton coupling in DNA hairpins composed of AT base pairs. Using Eq. **1** and experimental data for C_{12}-linked DNA hairpins, we estimated the exciton coupling between adjacent AT pairs in DNA as $V_0 \approx 0.035$ eV, which agrees with the semiempirical calculations (10).

Model

In this section we define the model for calculation of absorbance $A(E)$ and circular dichroism $\Theta(E)$ spectra by using the Fermi Golden rule (19). Circular dichroism is determined by the difference between absorbances $\delta A(E)$ of left-hand and right-hand

Author contributions: A.L.B. designed research; A.L.B., M.H., and F.D.L. performed research; A.L.B., M.E.A., M.H., and F.D.L. analyzed data; and A.L.B. wrote the paper.

The authors declare no conflict of interest.

This article is a PNAS Direct Submission.

[1]To whom correspondence should be addressed. E-mail: aburin@tulane.edu.

circularly polarized waves, which can be described by their vector potentials $\boldsymbol{A}_{l,r}(\boldsymbol{r},t) = \mathrm{Re}(A_0 \exp(iqz - i\omega t)(\boldsymbol{e}^x \mp i\boldsymbol{e}^y)$ for left- and right-hand polarized waves, respectively. Here, A_0 is the amplitude of the wave propagating in the z direction, ω and $q = n_r\omega/c$ are frequency and wavevector, n_r is the medium refractive index, and c is the speed of light. $\boldsymbol{e}_x$ and $\boldsymbol{e}_y$ are unit vectors in x and y directions. The ellipticity angle $\Theta(E)$ (in radians) used to characterize CD spectra can be expressed through the absorbance difference $\delta A(E)$ as $\Theta(E) = \ln(10)\delta A(E)/4$.

Molecules absorb optical energy because of their interaction with light (20)

$$\widehat{V}_{l,r} = -\frac{1}{c}\int d\boldsymbol{r}\,\boldsymbol{A}_{l,r}(\boldsymbol{r})\widehat{\boldsymbol{j}}(\boldsymbol{r}), \qquad [2]$$

where $\widehat{\boldsymbol{j}}(\boldsymbol{r})$ stands for the operator of an electron current density. For a polymer molecule made of n monomers having no remarkable electronic overlap, one can express this interaction Eq. **2** as the sum of interactions with each monomer $i = 1, 2, \ldots n$

$$\widehat{V}_{l,r} = -\mathrm{Re}\left(\sum_{i=1}^{n}\frac{A_0 e^{iqz_i - i\omega t}}{c}\int d\boldsymbol{\rho}\, e^{iq\rho}\left(\widehat{j}_i^{\,x} \mp i\widehat{j}_i^{\,y}\right)\right). \qquad [3]$$

Here, $\boldsymbol{r}_i$ and z_i stand for the average coordinate of the monomer i and $\boldsymbol{\rho} = \mathbf{r} - \mathbf{r}_i$.

The absorbance of light with the photon energy $E = \hbar\omega$ by a sample of a thickness L with a concentration of solute molecules n_* in the linear regime can be expressed by using the Fermi Golden rule as

$$A_{l,r}(E) = \frac{2\pi^2}{\hbar}\frac{n_* L}{cn_r}\frac{E}{\omega^2}\sum_{i,j=1;a}^{n}\delta(E - E_a)e^{iq(z_i - z_j)} \left\langle\left((j_i^x \mp ij_i^y)(\boldsymbol{q})\right)_{0\alpha}\left((j_j^x \pm ij_j^y)(-\boldsymbol{q})\right)_{\alpha 0}\right\rangle, \qquad [4]$$

where $(j_i^p(\boldsymbol{q}))_{0a} = \int d\boldsymbol{\rho}\,\Psi_0^* e^{iq\rho}\widehat{j}_i^{\,p}(\boldsymbol{\rho})\Psi_a$, index a enumerates electronic excited states of the molecule, and wavefunctions Ψ describe molecular electronic eigenstates. Configurational average $\langle\ldots\rangle$ is made over different realizations of solvent environment with respect to each molecule.

The system absorbance can be determined ignoring small products $qz \sim q\rho \approx 0$ because the wavelength of light $\lambda = 2\pi/q$ is much larger than the molecular size. In this approximation there is no difference between right- and left-hand polarizations. After the averaging of Eq. **4** over molecular orientations with respect to the external electromagnetic field we get

$$A(E) = \frac{4\pi^2 n_{\mathrm{abs}} L}{3\ln(10)n_r\hbar c}E\sum_{i,j=1;a}^{n}\left\langle\delta(E - E_a)\boldsymbol{\mu}_i^{0a}\boldsymbol{\mu}_j^{a0}\right\rangle, \qquad [5]$$

where $\widehat{\boldsymbol{\mu}}_i = i\int d\boldsymbol{\rho}\widehat{\boldsymbol{j}}_i/\omega$ stands for the dipole moment operator of the monomer i and n_{abs} is the concentration of molecules in absorption measurements.

Circular dichroism shows up in the first order in $ql \ll 1$, where $l \sim 1$ nm is the molecular size. Below we expand Eq. **4** to the first order in ql. One can find 3 contributions associated with 2 different terms in the expansion $e^{iq(z_i - z_j) + iq(\rho - \rho')} - 1 \approx iq(z_i - z_j) + iq(\boldsymbol{\rho} - \boldsymbol{\rho}')$. Both the first and second terms can be different for left- and right-hand polarized light and lead to the circular dichroism. The ellipticity angle determined by the difference of absorbances for right- and left-hand waves can be expressed after averaging over external field directions as

$$\Theta(E) = \Theta_1(E) + \Theta_2(E),$$

$$\Theta_1(E) = -\frac{\pi^2 n_{\mathrm{CD}} L}{3c\hbar^2}E^2 \times \sum_{i,j=1;a}^{n}\left\langle\delta(E - E_a)\boldsymbol{r}_{ij}\left(\boldsymbol{\mu}_i^{0a}\times\boldsymbol{\mu}_j^{a0}\right)\right\rangle,$$

$$\Theta_2(E) = -\frac{2\pi^2 n_{\mathrm{CD}} L}{3c\hbar^2}E^2 \times \sum_{i,j=1;a}^{n}\left\langle\delta(E - E_a)\left(\boldsymbol{i}_i^{0a}\boldsymbol{m}_j^{a0} + \boldsymbol{m}_i^{0a}\boldsymbol{i}_j^{a0}\right)\right\rangle. \qquad [6]$$

Here, n_{CD} is the concentration of molecules used in the circular dichroism measurements. The operator $\widehat{\boldsymbol{m}}_i = \frac{1}{2c}\int \boldsymbol{\rho}\times\widehat{\boldsymbol{j}}_i d\boldsymbol{\rho}$ stands for the monomer magnetic moment and the current operator $\widehat{\boldsymbol{i}}_i$ is the derivative of the dipole moment operator, so that $\boldsymbol{i}_i^{0a} = -\boldsymbol{i}_i^{a0} = i\omega\boldsymbol{\mu}_i^{0a}$.

The sum rules can be derived from Eqs. **5** and **6**. Before considering sum rules we define the model for the molecule.

The exciton Hamiltonian of a polymer molecule can be described by using the tight binding model coupled to the environment leading to fluctuations of monomer excitation energies ϕ_i. It can be written as (13)

$$\widehat{H}_0 = \sum_{i\neq j}V_{ij}c_i^+c_j + \sum_{i=1}^{n}\phi_i c_i^+c_i. \qquad [7]$$

Here, c_i, c_i^+ are operators of creation and annihilation of the exciton in a site (monomer) i. Random excitation energies ϕ_i can be characterized by their configurational averages $\varphi_i = \langle\phi_i\rangle$ and a distribution function $P(\phi_1, \phi_2, \ldots \phi_n)$. Interaction V_{ij} characterizes exciton coupling of monomers i and j. This coupling is most important for adjacent monomers. Since the distance between monomers is often comparable to their size (as in DNA) it must include various multipole interactions and cannot be reduced to the dipole–dipole interaction.

All monomers $i = 1, 2, \ldots, n$ possess transition dipole moments $\boldsymbol{\mu}_i$ and magnetic moments $\boldsymbol{m}_i$ having identical absolute values μ_0, m_0. The operators of transition dipole moments entering definitions Eqs. **5** and **6** can be expressed as

$$\widehat{\boldsymbol{\mu}}_i = \boldsymbol{\mu}_i(c_i^\dagger + c_i),\ \widehat{\boldsymbol{m}}_i = \boldsymbol{m}_i(c_i^\dagger - c_i). \qquad [8]$$

Our model is applicable when the electronic excitation of interest is well separated in energy from other electronic excitations. The overlap of absorption and CD spectra can be ignored when the energy difference Δ between this and the next electronic states exceeds inhomogeneous broadening

$$\Delta \gg W. \qquad [9]$$

The interaction of excitation with quantum vibrational modes $\hbar\omega > k_BT$ can also be included into our consideration in the standard form (21) of the shift of vibrational equilibria for excited states. Since it does not affect our results for sum rules, we will ignore that interaction.

Results

Sum rules can be expressed as the relationships for various momenta of the absorbance and ellipticity angle functions Eqs. **5** and **6**. Consider the integral $\int_0^{+\infty} dEA(E)/E$ using the definition Eq. **5**. The integral can be evaluated as

$$\int_0^{+\infty} dE\frac{A(E)}{E} = \frac{4\pi^2 n_{\mathrm{abs}} L}{3\ln(10)n_r\hbar}\sum_{i,j=1;a}^{n}\langle\widehat{\boldsymbol{\mu}}_i^{0a}\widehat{\boldsymbol{\mu}}_j^{a0}\rangle. \qquad [10]$$

Using the definition of transition dipole moment operator Eq. **8** we got $\sum_a\langle\widehat{\boldsymbol{\mu}}_i^{0a}\widehat{\boldsymbol{\mu}}_j^{a0}\rangle = \mu_0^2\langle 0\,|\,c_ic_j^\dagger\,|\,0\rangle = \mu_0^2\delta_{ij}$, where δ_{ij} is the

Kronecker symbol (i.e., $\delta_{ij} = 1$ if $i = j$ and 0 otherwise). Then Eq. **10** takes the form

$$\int_0^{+\infty} dE \frac{A(E)}{E} = \frac{4\pi^2 n_{\text{abs}} L n \mu_0^2}{3 n_r \ln(10) \hbar}. \quad [11]$$

Next, consider the integral $\int_0^{+\infty} dE A(E)$. Similarly to the previous derivation one can evaluate it into the form

$$\int_0^{+\infty} dE A(E) = \frac{4\pi^2 n_{\text{abs}} L}{3 \ln(10) n_r^2 \hbar} \sum_{i,j=1;a}^{n} (\boldsymbol{\mu}_i \boldsymbol{\mu}_j) \times \langle 0 \,|\, c_i \,|\, a \rangle E_a \langle a \,|\, c_j^\dagger \,|\, 0 \rangle. \quad [12]$$

Since quantum states a are eigenstates of the system Hamiltonian one can rewrite the sum over states a in Eq. **12** as the double sum

$$\sum_a \langle 0 \,|\, c_i \,|\, a \rangle E_a \langle a \,|\, c_j^\dagger \,|\, 0 \rangle = \sum_{a,b} \langle 0 \,|\, c_i \,|\, a \rangle \langle a \,|\, \hat{H}_0 \,|\, b \rangle \langle b \,|\, c_j^\dagger \,|\, 0 \rangle. \quad [13]$$

Because of its invariance with respect to the basis a one can change it to the basis of single-site excitations $|i\rangle$. Then one can rewrite Eq. **12** as

$$\int_0^{+\infty} dE A(E) = \frac{4\pi^2 n_{\text{abs}} L}{3 \ln(10) n_r^2 \hbar} \sum_{i,j=1}^{n} \langle i \,|\, H_0 \,|\, j \rangle (\boldsymbol{\mu}_i \boldsymbol{\mu}_j) = \frac{4\pi^2 \mu_0^2 n_{\text{abs}} L}{3 \ln(10) n_r^2 \hbar} \left(n \langle \phi \rangle + \sum_{i \neq j} V_{ij} \cos(\varphi_{ij}) \right), \quad [14]$$

where φ_{ij} is the angle between transition dipole moments of ith and jth monomers and $\langle \phi \rangle$ is the average monomer absorption energy. It is convenient to consider the ratio of Eqs. **14** and **11**. This ratio can be expressed as

$$\frac{\int_0^{+\infty} A(E) dE}{\int_0^{+\infty} A(E) dE / E} = \langle \phi \rangle + \sum_{i \neq j} \frac{V_{ij} \cos(\varphi_{ij})}{n}, \quad [15]$$

where φ is twisting angle for adjacent monomers. This result coincides with the sum rule derived in ref. 17.

Since the interaction V_{ij} decreases rapidly with the distance r_{ij} one can assume that only nearest-neighbor exciton coupling $V_0 = V_{i,i+1}$ is important. Then one can express it as

$$\frac{\int_0^{+\infty} A(E) dE}{\int_0^{+\infty} A(E) dE / E} = \langle \phi \rangle + \frac{2(n-1) V_0 \cos(\varphi)}{n}. \quad [16]$$

This result is independent of inhomogeneous broadening and can be used to study exciton coupling in various polymer molecules made of identical monomers. The dependence on the number of monomers and their coupling is similar to the one for the maximum of a rescaled absorption $\beta(E) = A(E)/E$ (10). However, the shift of maximum in $\beta(E)$ depends on the correlations between different site energies and the shape of the distribution of their fluctuations. In the absence of correlations and for the Gaussian distribution of fluctuations the shift of maximum in $\beta(E)$ is twice as large as that in Eq. **16**. One should notice that in contrast to Eq. **16**, this shift can be sensitive to vibrational interaction.

Despite a stronger universality of the sum rule Eq. **16** compared with the maximum change described in ref. 10 it is more difficult to apply this method to real spectra because the effect of interest represents a small correction. The overlap with other absorption bands can be comparable to it because it is not associated with weak exciton coupling. We were not able to apply this sum rule to the absorption spectra of stilbene-linked hairpins (11) because the contribution of stilbene to the tails of integrals in Eq. **16** could not be neglected in contrast to its effect on the maximum position (10). The situation is better for circular dichroism spectra, where exciton coupling can be responsible for the major contribution.

Consider sum rules for CD spectra. First, we evaluate the integral $\int_0^{\infty} dE \Theta(E)/E^2$ by using Eq. **6**. Similarly to Eq. **10** only the diagonal term with $i = j$ contributes to this integral. There, diagonal term contribution in Θ_1 vanishes because the vector product of 2 identical vectors is equal to zero ($\boldsymbol{\mu}_i \times \boldsymbol{\mu}_i = 0$). The evaluation of the second term results in the expression

$$\int_0^{\infty} dE \frac{\Theta(E)}{E^2} = -\frac{4n\pi^2 n_{\text{CD}} L \boldsymbol{m}\boldsymbol{j}*}{3 n_r c \hbar^2}. \quad [17]$$

If dot products of the transition current (the transition dipole moment multiplied by the frequency) and the transition magnetic moment ($\boldsymbol{m}\boldsymbol{j}*$) for each monomer differ from 0, then the circular dichroism is determined mostly by individual monomers. We do not consider this situation, which can be handled by first-principle methods (22).

Further consideration is restricted to the case $\boldsymbol{m}\boldsymbol{j}* = \boldsymbol{m}\boldsymbol{\mu} = 0$ for each monomer. The latter condition can be fulfilled for the systems having a special symmetry. For instance, if the monomer has a planar geometry as in DNA, then its transition dipole moment can also be parallel to that plane, while the magnetic moment is perpendicular to that plane. This takes place for electronic excitations of interest in DNA base pairs as well as in some amino acids (2, 6). In these systems the CD spectrum is determined by monomer interaction and Eq. **17** takes the form

$$\int_0^{\infty} dE \frac{\Theta(E)}{E^2} = 0. \quad [18]$$

Second, we evaluate the integral $\int_0^{\infty} dE \Theta(E)/E$. This integral can be calculated similarly to Eq. **14**. After evaluation of matrix elements we get

$$\int_0^{\infty} dE \frac{\Theta(E)}{E} = -\frac{\pi^2 n_{\text{CD}} L}{3 c \hbar^2} \sum_{i \neq j} \boldsymbol{r}_{ij} V_{ij} \boldsymbol{\mu}_i \times \boldsymbol{\mu}_j - \frac{4\pi^2 n_{\text{CD}} L}{3 c \hbar^2} \sum_{i,j=1;a}^{n} V_{ij} \boldsymbol{j}_i \boldsymbol{m}_j. \quad [19]$$

Exciton coupling can be conveniently expressed through the ratio of Eqs. **19** and **14**. This ratio reads

$$\frac{\int_0^{+\infty} dE \frac{\Theta(E)}{E}}{\int_0^{+\infty} dE \frac{A(E)}{E}} = -\frac{\ln(10) n_{\text{CD}} n_r}{4 n n_{\text{abs}} c \hbar} \sum_{i \neq j} \boldsymbol{r}_{ij} V_{ij} \frac{\boldsymbol{\mu}_i \times \boldsymbol{\mu}_j}{\mu_0^2} - \frac{\ln(10) n_{\text{CD}} n_r}{n n_{\text{abs}} c \hbar} \sum_{i,j=1;a}^{n} V_{ij} \frac{\boldsymbol{j}_i \boldsymbol{m}_j*}{\mu_0^2}. \quad [20]$$

Further simplification is possible if all monomers have planar structure and these planes are parallel to each other, as in DNA. Then all dot products of matrix elements for transition currents and magnetic moments are zeros and only the first term survives in Eq. **20**. The second term can also be neglected compared with the first term when the distance between adjacent monomers exceeds their characteristic sizes. Assuming that the first condition is satisfied and leaving only nearest-neighbor interaction V_0 one can express the identity Eq. **20** in the form equivalent to Eq. **1**

$$\frac{\int_0^{+\infty} dE \frac{\Theta(E)}{E}}{\int_0^{+\infty} dE \frac{A(E)}{E}} = -\ln(10) \frac{n-1}{2n} \sin(\varphi) n_r \frac{n_{\text{CD}}}{n_{\text{abs}}} \frac{dV_0}{c\hbar}, \quad [21]$$

remember that the length d is the distance between adjacent monomers.

The identities Eqs. **21** and **16** are the main results of this work. Below we use them to determine the exciton coupling strength V_0 between AT base pairs in DNA and compare this result with

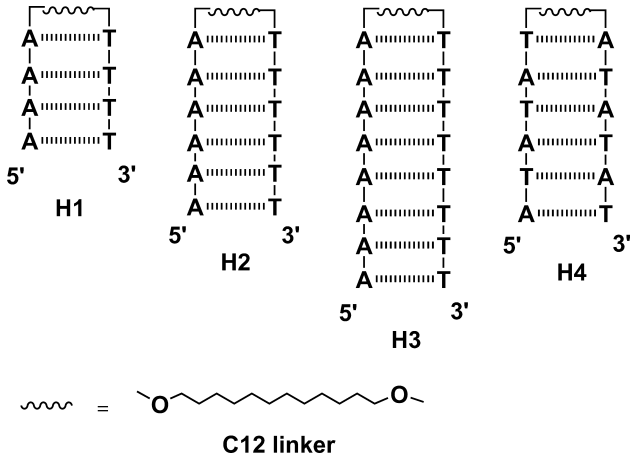

Fig. 1. Structure of C_{12}-linked DNA hairpins.

the numerical calculations and experimental definition by using a maximum in rescaled absorption spectrum (10).

Discussion

We discuss absorption and circular dichroism data in C_{12}-linked hairpins H1–H4 (Fig. 1). These hairpins are more convenient for optical measurements than stilbene-linked hairpins because, in contrast to stilbene, a C_{12} linker has no absorption band overlapping with the low energy absorption band of AT base pairs. The syntheses and characterization of hairpins H2 and H4 have recently been reported (23). A minimized structure for H2 obtained from molecular dynamics simulations is shown in Fig. 2. Salient features of this structure are the extended all-anti conformation of the alkane linker and the B-DNA structure of the base pair domain, which is similar to that recently reported for a hexa(ethylene glycol)-linked hairpin (24).

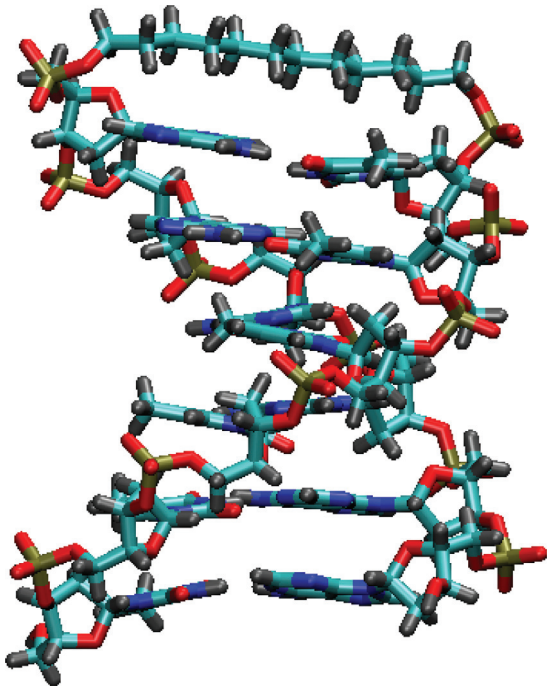

Fig. 2. A minimized structure for H2 obtained from molecular dynamics simulations (24).

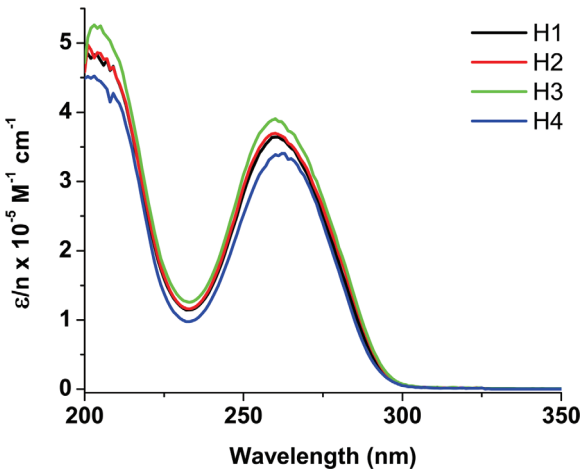

Fig. 3. Absorption spectra of C_{12}-linked hairpin sequences H1–H4 in 10 mM phosphate buffer (pH 7.2) containing 100 mM NaCl normalized for the number of base pairs.

The absorption spectra of the DNA hairpins are shown in Fig. 3. The absorbance per base pair decreases slightly with increasing length for hairpins H1 > H2 > H3 and is greater for the alternating sequence H4 vs. the homopolymeric sequence H2. These trends are consistent with increased hypochromism with increased A-tract length (25). The low-energy absorption peak at the wavelength 260 nm corresponds to the photon energy $E_1 \approx 4.5$ eV. It is separated from the next peak at $E_2 \approx 5.8$ eV by the energy on the order of 1 eV. Inhomogeneous broadening of the first peak estimated using the Gaussian fit is on the order of 0.4 eV so the peaks are separated. Therefore, one can try to use sum rules to determine the exciton coupling for electronic excitations, corresponding to the first peak.

Fig. 4 shows the CD spectra of hairpin sequences H1–H4. A careful analysis of the long-wavelength region (230–300 nm) of the CD spectrum provides a clear understanding on the contribution of the DNA bases on the first excited state. The positive Cotton effect with a zero crossing at 260 nm near absorption maximum could be attributed to the fact that the CD spectrum is determined by the difference of left- and right-hand polarized waves. Since the DNA double helix is right-handed and shorter wavelengths correspond to a nearly parallel orientation of dipole moments of interacting base pairs in a collective exciton state (10) the right-hand

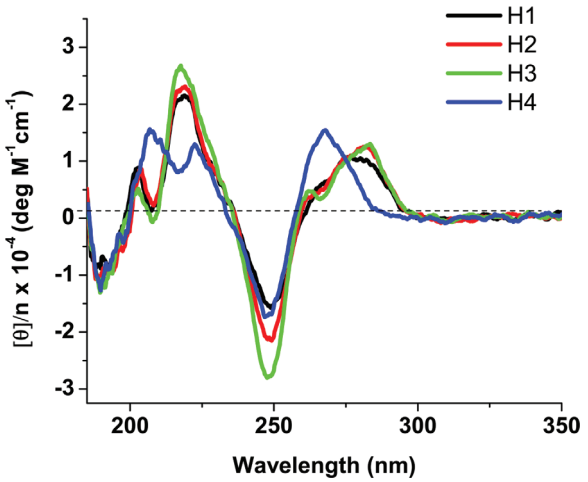

Fig. 4. Circular dichroism band of C_{12}-linked hairpin sequences H1–H4 in 10 mM phosphate buffer (pH 7.2) containing 100 mM NaCl normalized for the number of base pairs.

polarized wave will be absorbed more strongly here. Therefore, the difference between absorptions of left- and right-hand polarized waves is negative. However, the longer wavelength region of the spectrum contains dipole moments of different base pairs that are oriented nearly opposite to each other, which leads to the stronger absorption of left-hand polarized waves and consequently positive Cotton effect.

The experimental data for ellipticity angle Ψ in Fig. 4 are given in millidegrees. One can reexpress the identity Eq. **1** in terms of experimental units using the definition $\Psi = \Theta \cdot 180 \cdot 1000/\pi$, DNA parameters $\varphi = 36^\circ$ for poly(A)–poly(T) sequences ($H1, H2, H3$) and $d = 3.4A$, water refractive index $n_r = 1.33$ and experimental ratio $n_{abs}/n_{CD} \approx 10$ as

$$V_0(\text{eV}) \approx -0.11 \frac{n}{n-1} \frac{\int_0^{+\infty} dE\Psi(E)/E}{\int_0^{+\infty} dEA(E)/E}. \quad [22]$$

Exciton coupling V_0 is expressed in electron volts.

To estimate the exciton coupling strength Eq. **22** one has to perform the numerical integration of absorption and CD spectra (Figs. 3 and 4) over the part of the spectrum associated with the first electronic excited state, i.e., the longest-wavelength absorption band. This band is essentially symmetric with respect to the maximum until large energies on the order of 5.1 eV (short wavelengths), where other electronic excitations become important. The part of the absorption spectrum on the long-wavelength side of the maximum is less affected by other excitations. Therefore one can estimate the integral in the denominator of Eq. **22** as the doubled integral over the low-energy (long-wavelength) side. Performing the integration we evaluated $I_X^{abs} = \int_0^{+\infty} dEA(E)/E$ as $I_{H1} \approx 0.156$, $I_{H2} \approx 0.17$, $I_{H3} \approx 0.168$, $I_{H4} \approx 0.14$ (see Fig. 1 for definitions of DNA hairpins $H1$, $H2$, $H3$, and $H4$).

We assumed that the first bright electronic excitation of AT pair can be approximately separated from other excitations at least for the lower-energy part of the spectrum. This expectation is justified by our calculations of AT pair excitation spectrum preliminary reported in ref. 10. According to these calculations there is the one lowest energy bright state at the excitation energy 4.2 eV. This is a reasonable estimate for the observed absorption peak at 4.5 eV. Next bright excited state of AT pair has been found at energy 0.3 eV higher. Therefore, we assume that the Cotton effect is due to the lowest-energy bright transition and the contribution of the second transition can be almost ignored for the low-energy wing of the CD band. Although separate A and T bases have almost identical excitation energies of their first bright excited states (see refs. 26 and 27, and references therein) the situation can be different for AT pairs, for instance, due to electrostatic interactions of A and T bases. Below, the reasonable agreement of estimates for exciton coupling of adjacent AT pairs obtained using sum rules and numerical calculations is demonstrated. This agreement also supports our consideration of a single transition. The additional features in the CD band, including the inflections around 265 nm, can be due to the next-neighboring AT pair interactions; their analysis is beyond the accuracy of our approach.

It is more difficult to estimate the integral over the ellipticity angle in the numerator in Eq. **22**. Its short-wavelength (high-energy) part is clearly affected by high-energy electronic excitations. To evaluate it approximately, using only the low-energy part of the spectrum similarly to the absorption spectrum, one can redefine variables as $E = E_0 + \xi$, where E_0 is the energy of spectrum maximum E_0 corresponding to the zero circular dichroism. Then, the integral reads

$$\int_{-\infty}^{+\infty} d\xi \frac{\Psi(E_0+\xi)(E_0+\xi)}{(E_0+\xi)^2} = E_0 \int_{-\infty}^{+\infty} d\xi \frac{\Psi(E_0+\xi)}{(E_0+\xi)^2} + \int_{-\infty}^{0} d\xi \frac{\Psi(E_0+\xi)\xi}{(E_0+\xi)^2} + \int_{0}^{+\infty} d\xi \frac{\Psi(E_0+\xi)\xi}{(E_0+\xi)^2}. \quad [23]$$

The first term in Eq. **23** is equal to zero according to the identity Eq. **18**. Two remaining integrals must be approximately equal to each other for the single electronic excitation according to the perturbation theory (13, 14) for symmetric absorption spectra. Since the absorption spectrum density $A(E)/E$ is approximately symmetric with respect to its maximum at $E = E_0$ and the perturbation theory (13) in V/W should be applicable for $W \sim 0.4$ eV and $V_0 \sim 0.05$ eV (10) one can approximate the integral in the numerator of the identity in Eq. **22** as

$$\int_0^{+\infty} dE \frac{\Psi(E)}{E} \approx 2 \int_{-\infty}^{0} d\xi \frac{\Psi(E_0+\xi)\xi}{(E_0+\xi)^2}. \quad [24]$$

Numerical evaluation of integrals for different hairpins (Fig. 1) yields $I_{H1}^{CD} \approx -0.0368$, $I_{H2}^{CD} \approx -0.045$, $I_{H3}^{CD} \approx -0.0433$, $I_{H4}^{CD} \approx -0.024$.

Using these results one can estimate exciton coupling for different hairpins. The first 3 hairpins $H1$, $H2$, and $H3$ are poly(A)–poly(T) sequences of n AT pairs with $n = 4$, 6 and 8, respectively. Using Eq. **22** we obtained three estimates $V_0^{H1} = 0.035$ eV, $V_0^{H2} = 0.036$ eV, and $V_0^{H3} = 0.033$ eV. The average coupling $V_0 = 0.035$ eV is close to the result of semiempirical INDO calculations using Gaussian software (22) $V_0 \approx 0.04$ eV reported in ref. 10, which is a reasonably good agreement.

The fourth hairpin $H4$ is made of $n = 6$ alternate AT-TA base pairs. Exciton coupling of nearest neighbors AT-TA should differ from AT-AT coupling V_0 estimated above. Indeed we obtained $V_0^{TA,AT} \approx 0.023 \cdot \sin(36^\circ)/\sin(\varphi')$ eV, where φ' is the angle between transition dipole moments of adjacent AT and TA pairs. It is not surprising that $V_0^{TA,AT} < V_0$ because the distance between electronic excitations is larger in the alternate sequence. The exciton coupling $V_0^{TA,AT}$ and the angle φ' were estimated using INDO method similarly to ref. 10 as $V_0^{TA,AT} = 0.021$ eV, $\sin(\varphi') \sim 0.64$. This estimate agrees very well with the one based on the sum rules. Thus, our theoretical analysis is consistent with the calculations of exciton coupling.

Conclusion

In this article we derived the sum rules for absorption and circular dichroism spectra of polymer molecules. Using these sum rules one can express exciton coupling strength through the integral properties of absorption and CD spectra. This result can be used in the experimental investigation of structural changes in biological molecules during chemical or biological processes.

The results are insensitive to the inhomogeneous broadening. However, they are applicable only if other electronic excited states are well separated from the state under consideration.

Using the sum rules applied to DNA hairpin absorption and CD spectra, we estimated exciton coupling between AT-AT and AT-TA base pairs to be 0.035 eV and 0.023 eV, respectively. This result agrees with the numerical calculations. This analysis can be easily generalized to other DNA conformations. Thus our method establishes the direct link between absorption and CD spectra, and DNA structural and conformational changes through exciton coupling strength of base pairs. This link can be used to investigate chemical and biological processes involving DNA using optical methods.

ACKNOWLEDGMENTS. We thank Igor Tupitzyn and Russ Schmehl for referring us to the Van Vleck identity and sum rules for absorption, Martin McCullagh and George Schatz for providing Fig. 2, Torsten Fiebig, George Schatz, Carleigh Hebbard, Amy Finch, Balamurugan Desinghu, Stefano Tonzani, and Scott Knowles for useful discussions, critical comments, and suggestions. This work was supported by the National Science Foundation Collaborative Research in Chemistry Program Grant 0628092.

1. Merino EJ, Boal AK, Barton JK (2008) Biological contexts for DNA charge transport chemistry. *Curr Opin Chem Biol* 12:229–237.
2. Fasman GD, ed (1996) *Circular Dichroism and the Conformational Analysis of Biomolecules* (Plenum Press, New York).
3. Lightner DA, Gurst JE (2000) *Organic Conformational Analysis and Stereochemistry from Circular Dichroism Spectroscopy* (Wiley-VCH, New York).
4. Wouters FS, Verveer PJ, Bastiaens PIH (2001) Imaging biochemistry inside cells. *Trends Cell Biol* 11:203–211.
5. Moerner WE (2002) Single-molecule optical spectroscopy of autofluorescent proteins. *J Chem Phys* 117:10925–10937.
6. Lightner DA, Gurst JE (2000) *Organic Conformational Analysis and Stereochemistry from Circular Dichroism Spectroscopy* (Wiley-VCH, New York).
7. Tinoco I Jr (1960) Hypochromism in polynucleotides. *J Am Chem Soc* 82:4785–4790.
8. Turro NJ, Barton JK, Tomalia DA (1991) Molecular recognition and chemistry in restricted reaction spaces. Photophysics and photoinduced electron transfer on the surfaces of micelles, dendrimers, and DNA. *Acc Chem Res* 24:332–340.
9. Yaney P, Heckman E, Diggs D, Hopkins F, Grote J (2005) Development of chemical sensors using polymer optical waveguides fabricated with DNA. *Proc SPIE* 5724:224–233.
10. Burin AL, Dickman JA, Uskov DB, Hebbard CFF, Schatz GC (2008) Optical absorption spectra and monomer interaction in polymers. Investigation of exciton coupling in DNA hairpins. *J Chem Phys* 129:091102.
11. Lewis FD, *et al*. (2005) DNA as helical ruler: Exciton-coupled circular dichroism in DNA conjugates. *J Am Chem Soc* 127:14445–14453.
12. Onidas D, Gustavsson T, Lazzarotto E, Markovitsi D (2007) Fluorescence of the DNA double helix $(dA)_{20}$-$(dT)_{20}$ studied by femtosecond spectroscopy—Effect of the duplex size on the properties of the excited states. *J Phys Chem B* 111:9644–9650.
13. Balamurugan D, Lewis FD, Burin AL (2007) Circular dichroism spectra of DNA hairpins studied by the green function method. *J Phys Chem* 111:3982–3989.
14. Kamiya M (1987) An extended theoretical formulation of the circular dichroism band shape of chromophore aggregates by use of the ensemble-averaged resolvent matrix method. *J Chem Phys* 86:5308–5314.
15. Eisfeld A, Kniprath R, Briggs JS (2007) Theory of the absorption and circular dichroism spectra of helical molecular aggregates. *J Chem Phys* 126:104904.
16. Van Vleck JH (1948) The dipolar broadening of magnetic resonance lines in crystals. *Phys Rev* 74:1168–1183.
17. Briggs JS, Herzenberg A (1970) Sum rules for the vibronic spectra of helical polymers. *J Phys B Atom Mol Phys* 3:1663–1676.
18. Joens JA (1993) Sum rule methods for the approximation of continuous electronic absorption spectra. *J Phys Chem* 97:2521–2534.
19. Landau LD, Lifshitz EM (1981) *Quantum Mechanics: Non-Relativistic Theory* (Butterworth-Heinemann, Boston), 3rd Ed.
20. Landau LD, Lifshitz EM (1980) *The Classical Theory of Fields* (Butterworth-Heinemann, Boston), 4 Ed.
21. Marcus RA (1993) Electron transfer reactions in chemistry. Theory and experiment. *Rev Mod Phys* 65:599–610.
22. Frisch MJ, *et al.* (2004) *Gaussian* 03 (Gaussian, Inc., Wallingford CT), Revision C.02.
23. Hariharan M, Lewis FD (2008) Context-dependent photodimerization in isolated thymine-thymine steps in DNA. *J Am Chem Soc* 130:11870–11871.
24. McCullagh M, *et al.* (2008) Effect of loop distortion on the stability and structural dynamics of DNA hairpin and dumbbell conjugates. *J Phys Chem B* 112:11415–11421.
25. Cantor CR, Schimmel PR (1980) *Biophysical Chemistry* (W. H. Freeman, New York).
26. Bouvier B, Gustavsson T, Markovitsi D, Milli P (2002) Dipolar coupling between electronic transitions of the DNA bases and its relevance to exciton states in double helices. *Chem Phys* 275:75–92.
27. Onidas D, Gustavsson T, Lazzarotto E, Markovitsi D (2007) Fluorescence of the DNA double helix $(dA)_{20}(dT)_{20}$ studied by femtosecond spectroscopy—Effect of the duplex size on the properties of the excited states. *J Phys Chem B* 111:9644–9650.